



Cite this: Analyst, 2017, 142, 2378

## Glass capillary based microfluidic ELISA for rapid diagnostics†

Xiaotian Tan, <sup>a</sup> Maung Kyaw Khaing Oo, <sup>a</sup> Yuan Gong, <sup>a,c</sup> Yaxin Li, <sup>b</sup> Hongbo Zhu<sup>a</sup> and Xudong Fan \*<sup>a</sup>

Enzyme-linked immunosorbent assay (ELISA) is widely used in medical diagnostics and fundamental biological research due to its high specificity and reproducibility. However, the traditional 96-well-plate based ELISA still suffers from several notable drawbacks, such as long assay time (4–6 hours), burdensome procedures and large sample/reagent volumes (~100 µL), which significantly limit traditional ELISA's applications in rapid clinical diagnosis and quasi-real-time prognosis of some fast-developing diseases. Here, we developed a user friendly glass capillary array based microfluidic ELISA device. Benefiting from the high surface-to-volume ratio of the capillary and the rapid chemiluminescent photo-imaging method with a commercial camera, our capillary based ELISA device significantly reduced the sample volume to 20 µL and shortened the total assay time to as short as 16 minutes (including detection time), which represent approximately 10-fold and 5-fold reduction in assay time and sample volume, respectively, in comparison with the traditional plate-based method. Furthermore, through the double exposure method, a nearly 10-fold increase in the detection dynamic range was achieved over the traditional well-based ELISA. Our device can be broadly used in rapid biochemical analysis for biomedicine and research/development laboratories.

Received 27th March 2017,  
Accepted 14th May 2017

DOI: 10.1039/c7an00523g  
[rsc.li/analyst](http://rsc.li/analyst)

## Introduction

In the past few decades, various types of immunoassays have been increasingly used in identifying and quantifying biomarkers and pathogens. Among all, enzyme linked immunosorbent assay (ELISA) has become one of the most popular immunoassays due to its high specificity and reproducibility. To some extent, it has been regarded as a “gold standard” for quantifying analytes in both medical diagnostics and fundamental biological research.<sup>1,2</sup> However, traditional (96-well plate based) ELISA still suffers from several notable drawbacks, such as long assay time (4–6 hours), burdensome procedures, and large sample/reagent consumption (~100 µL).<sup>1,3</sup> Although signal detection has been continuously simplified through techniques such as smartphone imaging,<sup>4–7</sup> these inherent disadvantages still significantly limit traditional ELISA's appli-

cations in the areas such as rapid clinical diagnosis and quasi-real-time prognosis of certain diseases, especially for fast-developing severe illnesses (*e.g.*, sepsis, acute organ rejection, and myocardial infarction).

Advances in microfluidic techniques provide a promising solution to address the aforementioned problems. The feasibility of performing ELISA in an integrated microfluidic system such as a PDMS chip,<sup>4,8–11</sup> polystyrene chip,<sup>4,12</sup> and centrifugal disc<sup>13–15</sup> has been demonstrated. Magnetic and polystyrene microbeads were also employed in a few other kinds of microfluidic ELISA devices.<sup>9,16–18</sup> However, most of these approaches involve sophisticated fluidic designs and usually suffer from low multiplexed capacity, insufficient rinsing (due to residual liquids), low repeatability, strong background, small dynamic range, and low signal-to-noise ratios.<sup>9,19</sup> Furthermore, despite the use of microfluidics, the entire device still requires expensive equipment such as a fluorescent microscope<sup>9</sup> or a photomultiplier tube (PMT) equipped reader<sup>20</sup> to take measurement. Consequently, a practically feasible and inexpensive ELISA device with simple design, high speed, high sensitivity, large dynamic range, low sample/reagent consumption, and multiplexed capability is highly desirable.

Benefitting from the high surface-to-volume ratio, small sample consumption, and structural simplicity, capillaries provide another microfluidic platform for ELISA. Over the past few years, the standard or simplified versions of ELISA have

<sup>a</sup>Department of Biomedical Engineering, University of Michigan, 1101 Beal Ave., Ann Arbor, MI 48109, USA. E-mail: [xsfan@umich.edu](mailto:xsfan@umich.edu)

<sup>b</sup>Department of Chemistry, University of Michigan, 1101 Beal Ave., Ann Arbor, MI 48109, USA

<sup>c</sup>Key Laboratory of Optical Fiber Sensing and Communications, University of Electronic Science and Technology of China, No. 2006, Xiyuan Ave., Chengdu, 611731, P. R. China

† Electronic supplementary information (ESI) available. See DOI: [10.1039/c7an00523g](https://doi.org/10.1039/c7an00523g)

been carried out using thin microfluidic glass capillaries ( $0.1\text{ mm} \times 0.1\text{ mm}$  for inner dimensions, wall thickness  $0.1\text{ mm}$ ), showing that the immunoassay can be quantified either fluorescently or colorimetrically with a fluorescent microscope<sup>21–24</sup> or a transmitting light detector.<sup>25</sup> However, in these capillary systems, samples and reagents are delivered *via* the capillary force, which is difficult to control. Consequently, they suffer from low repeatability, low reliability, high background (due to the incomplete rinse of the liquid residuals at the capillary corners), and low sensitivity and dynamic range. Moreover, since fluorescent or colorimetric substrates are used in these systems, additional 15–30 minutes of enzyme–substrate reaction time is needed to generate a detectable signal, which is a bottleneck for further reduction in total assay time.

Here we developed a user friendly glass capillary based microfluidic ELISA device. The capillaries were chemically pre-activated before starting a sandwich ELISA. Thanks to the high surface-to-volume ratio of the capillary ( $4\text{ mm}^{-1}$  vs.  $0.32\text{ mm}^{-1}$  for a typical well in a 96-well plate) and the rapid chemiluminescent imaging method (with a commercial camera), this technique significantly reduced the sample volume to  $20\text{ }\mu\text{L}$  and shortened the total assay time to around 16 minutes (including the final chemiluminescence measurement), which is considerably faster and simpler than the existing microfluidic approaches. In comparison with the traditional ELISA using 96-well plates, our capillary based microfluidic ELISA has an approximately 10-fold reduction in assay time, 5-fold reduction in sample/reagent consumption volumes, and about 10-fold enhancement in the dynamic range (from 2.5 to ~4 orders of magnitude), while maintaining comparable sensitivity.

## Materials and methods

### Materials

The chemiluminescent substrate (SuperSignal™ ELISA Femto Substrate) was purchased from Thermo Fisher. The substrate kit (product no. 37075) contains a bottle of  $50\text{ ml}$  Luminol + Enhancer Solution and a bottle of  $50\text{ ml}$  Stable Peroxide Solution. The working substrate solution was prepared by equal-volumetrically mixing the Luminol + Enhancer Solution and the Stable Peroxide Solution at room temperature. The human serum (from human male AB plasma) used in this experiment was purchased from Sigma-Aldrich (product number H4522). The reagents used for surface activation, 3-APTMS, toluene and methanol, were purchased from Sigma-Aldrich.

For interleukin-6 (IL-6) ELISA, human IL-6 DuoSet ELISA Kit (DY206), ELISA plate-coating buffer ( $1\times$  PBS, DY006), wash buffer (WA126) and reagent diluent (10% BSA in  $10\times$  PBS, DY995) were purchased from R&D Systems. The stock solutions of the capture antibody, detection antibody and human IL-6 standard were prepared according to the procedure described in the kits' user manual. The working solution of wash buffer and reagent diluent were diluted with Milli-Q water ( $R = 18.2\text{ }\Omega$ ) to achieve  $1\times$  working concentration. The  $1\times$  reagent

dilute solution (1% BSA in PBS) was further used as a blocking buffer. In this set of experiment, the capture antibody stock solution was diluted with PBS buffer and finally achieved a concentration of  $10\text{ }\mu\text{g ml}^{-1}$  (working concentration). The working solution of the biotinylated detection antibody was prepared by diluting the stock solution with the  $1\times$  reagent diluent and finally achieved an antibody concentration of  $0.3\text{ }\mu\text{g ml}^{-1}$  (the detection antibody was biotinylated by the manufacturer). The concentrated human IL-6 standard was diluted to a desired concentration with the  $1\times$  reagent diluent or human serum (H4522). The working solution of the streptavidin-HRP conjugate (SAv-HRP) was prepared by diluting the stock solution (included in the DY206 kit) to  $1/20$  of its original concentration (with the  $1\times$  reagent diluent). The concentrations of the working solutions were identical for both capillary based and 96-well plate based ELISA.

For CK-MB ELISA, the CK-MB protein standard (AKC0325) was purchased from Thermo Fisher. A mouse monoclonal antibody (ab19603) and a goat polyclonal antibody (ab110655) were used as the capture antibody and the detection antibody, respectively, both of which were purchased from Abcam. The same as the IL-6 experiments, the stock solution of ELISA plate-coating buffer (DY006), wash buffer (WA126) and reagent diluent (DY995) were purchased from R&D Systems. The working solution of the wash buffer and reagent diluent were diluted with Milli-Q water ( $R = 18.2\text{ }\Omega$ ) to achieve  $1\times$  working concentration. In CK-MB experiments,  $2\times$  reagent dilute solution (2% BSA in PBS) was used as the blocking buffer. The working solution of the capture antibody was prepared by diluting the stock solution with PBS buffer to achieve a final concentration of  $8\text{ }\mu\text{g ml}^{-1}$ . The concentrated human CK-MB standard was diluted to a desired concentration with the  $1\times$  reagent diluent or human serum (H4522). Since the detection antibody was not pre-conjugated with biotin or a reporter enzyme, it was modified by conjugating with HRP in a molar ratio of antibody:HRP =  $1:4$ . The conjugation reaction was performed covalently with Abcam's HRP conjugation kit (ab102890). The concentration of the HRP-conjugated detection antibody stock solution was  $1\text{ mg ml}^{-1}$ . It was further diluted with the  $1\times$  reagent diluent and finally achieved a working antibody concentration of  $0.7\text{ }\mu\text{g ml}^{-1}$ . The concentrations of the working solutions were identical in both capillary based and plate based ELISA assays.

The borosilicate glass capillaries ( $1\text{ mm} \times 1\text{ mm}$  inner cross section,  $150\text{ }\mu\text{m}$  wall thickness, and  $30.5\text{ cm}$  in length) were purchased from Friedrich & Dimmock and then cut into  $4\text{ cm}$  long pieces with a ceramic wafer. The volume of the entire capillary was  $40\text{ }\mu\text{l}$ . During our experiments, we used only a half of it (*i.e.*,  $20\text{ }\mu\text{l}$ ).

### Preparation of capillary reactors

In order to reduce the impact of liquid residue at the corners of reactors and increase the signal intensity generated in each capillary, we decided to use capillary reactors with relatively large interior dimensions ( $1\text{ mm} \times 1\text{ mm}$ ). Fig. 1A and B show the exterior appearance of capillary ELISA reactors. In order to

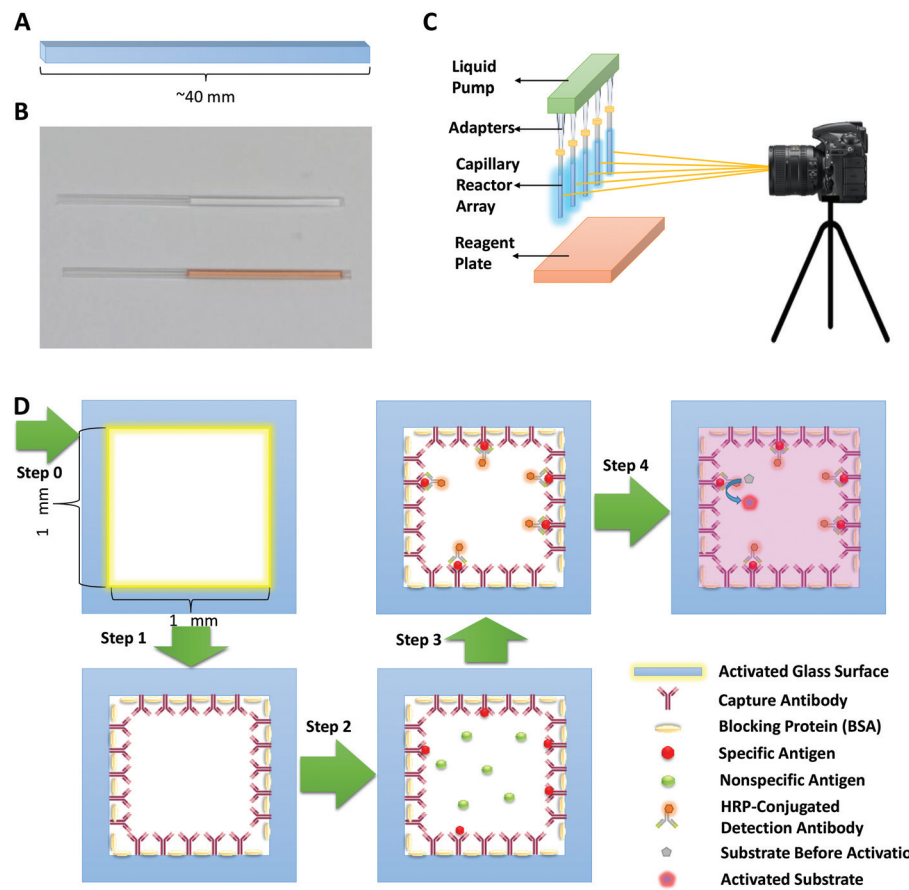


**Fig. 1** (A) Schematic of a glass capillary based ELISA reactor. (B) Picture of capillary ELISA reactors with an unreacted chemiluminescent substrate (top) and a fully reacted chemiluminescent substrate (bottom). (C) Schematic of the experimental setup. A 12-channel pipette was used as a liquid pump, pipette tips were used as adapters, PCR tubes were used as sample/reagent reservoirs, a Canon 80D SLR camera was used as an imager. (D) Procedures for running ELISA in a glass capillary. Step 0: Surface activation; Step 1: Capture antibody immobilization and surface blocking. Step 2: Sample addition and incubation. Step 3: Detection antibody addition and incubation. Step 4: Substrate addition and measurement.

improve the protein affinity of the capillaries, we performed surface chemical activation on the capillary inner surface, as illustrated in Fig. S1.<sup>†</sup> The activation process is composed of three steps: (1) Treatment with air plasma for 5 minutes with a plasma etching machine (for cleaning and hydroxylation). (2) Incubate with 20 mM 3-APTES toluene solution overnight (for anchoring a layer of 3-APTES). (3) Rinse with toluene and methanol (for removal of unbounded 3-APTES). The activated glass surface is coated with a layer of primary amino groups, which are reactive with the free carboxyl groups that can be found on aspartic acid, glutamic acid, and the C-terminus of proteins. Since the amount of free carboxyl groups is limited by the number of available amino acids, this approach will generate a modest, but not overly strong affinity toward proteins, thus lowering the risk of non-specific bindings. The capillaries can be batch-processed (up to 200 capillaries per batch) to ensure the consistency in surface activation and subsequent ELISA. The surface activated capillaries are stable and can be stored at room temperature (soaked in deionized water) for over two months without reduction in protein affinity. The details of the capillary reactor and its dimensions can be

found in Fig. S2.<sup>†</sup> The activated capillaries were then glued onto pipette tips (Fisherbrand 200 µl pipette tips). The structure of a typical capillary reactor is illustrated in Fig. S2A.<sup>†</sup> 12 capillary reactors were then connected with a liquid pump (in this case, a Scilogex 5–50 µl 12-channel pipette) to form a capillary reactor array.

#### Experimental setup

A schematic diagram of the experimental setup is shown in Fig. 1C. For chemiluminescent imaging, a Canon 80D SLR camera equipped with a Canon EF 100 mm f/2.8L Macro IS USM Lens was used as an image detector. When taking measurement, the camera was connected to a tripod and placed 45 cm from the focal plane (the distance from the lens to capillaries). Owing to the adjustable negative pressure generated by the multi-channel pipette, the capillaries can accurately draw liquid from the reagent plate and maintain the liquid level. Consequently, the entire assay, including incubation, rinsing, and measurement can all be performed when the capillaries are positioned vertically. During the assay, we usually drew only 20 µl of samples/reagents into the capillary.

Fig. 1D illustrates a detailed schematic of a standard sandwich ELISA performed in a glass capillary reactor. The reaction contains 4 steps: (1) Capture antibody immobilization and surface blocking. (2) Sample addition and incubation. (3) Detection antibody addition and incubation. Note that in this step if the detection antibody is not pre-conjugated with reporter enzymes such as HRP (horseradish peroxidase), an additional step for enzyme conjugation is needed. (4) Substrate addition and final measurement with the camera. The time for steps 1–3 may vary, depending on the analytes. Between two adjacent steps, waste liquid discharge and 4 times of rinsing with wash buffer are carried out.

## Results and discussion

Unlike fluorescent or colorimetric substrates that require 15–30 minutes of reaction time to generate adequate signals, a chemiluminescent ELISA substrate can generate detectable optical signals immediately after it reacts with the reporter enzyme (HRP, in this work) conjugated on the detection antibody. The emission intensity of the SuperSignal™ substrate

remains steady for several minutes. Therefore, the signal intensity during this plateau period can be quantified by the imaging method with a camera.

According to the emission spectrum shown in Fig. 2A, a large portion of the emitting light has a wavelength between 375 nm and 525 nm. Fig. 2B describes the procedure to generate analyzable data from an image. In order to enhance the signal intensity and reduce unrelated background noises, only the signal from the blue channel, which covers the spectral range of 420–520 nm, was analyzed. To avoid the potential disturbance caused by light reflection at the capillary edges, only the intensity along the central axis of each capillary was recorded and then averaged along the capillary longitudinal direction.

The capillary based microfluidic ELISA system was evaluated with several clinically important biomarkers. We first chose to use human IL-6, which is a widely-used indicator of inflammatory response status and also a marker for immunological diseases such as sepsis and acute organ rejection.<sup>26,27</sup> The corresponding ELISA protocol is illustrated in Fig. 3A. Note that, since the detection antibody provided in the commercial IL-6 ELISA kit was only biotinylated but not pre-conju-

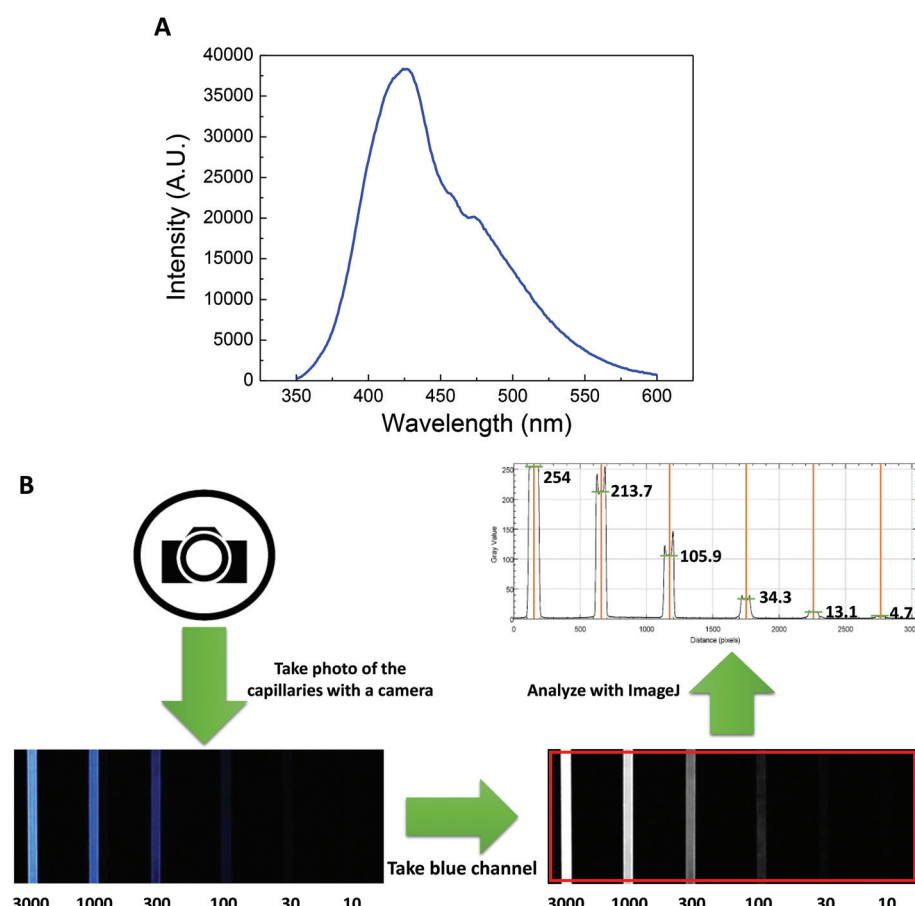
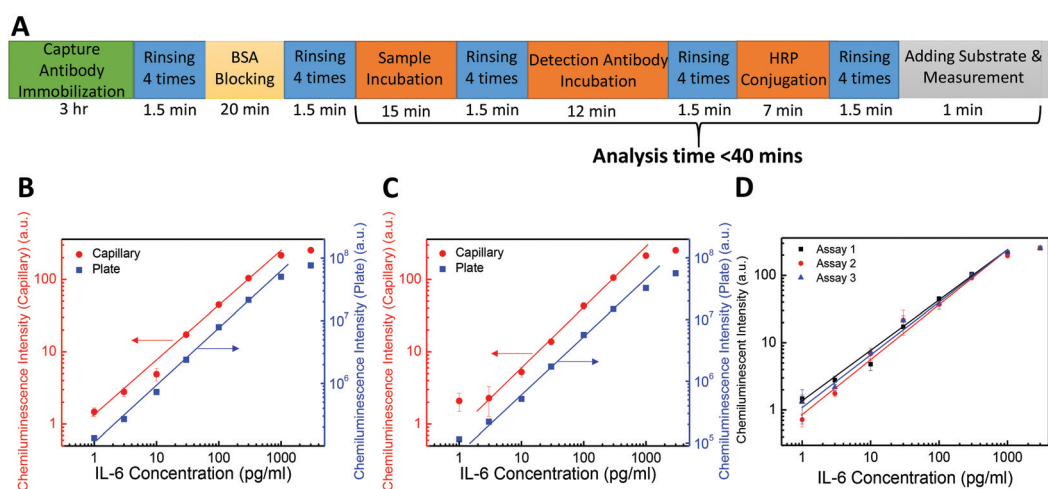


Fig. 2 (A) Emission spectrum of the SuperSignal™ chemiluminescent ELISA substrate (Luminol based substrate). (B) Procedures of signal quantification. The signal from the blue channel was extracted and analyzed. A plot profile of light intensity was generated with ImageJ. The red box indicates the light intensity measurement region. The numbers under each capillary are the corresponding IL-6 concentration in a sample (in units of  $\text{pg ml}^{-1}$ ).



**Fig. 3** (A) Protocol of running sandwich IL-6 ELISA in capillary reactors. The total assay time is less than 40 minutes. (B) ELISA measurement of IL-6 in buffer solution with capillary reactors and a 96-well plate. (C) ELISA of IL-6 in human serum with capillary reactors and a 96-well plate. (D) The performance of ELISA measurement of IL-6 in buffer solution in three different trials using capillary reactors. Red lines in B and C are the linear fit for the data collected with capillary reactors on the log–log scale with a slope of 0.7578 and 0.8117, respectively. Blue lines in B and C are the linear fit for the data collected with a 96-well plate on the log–log scale with a slope of 0.8966 and 0.8943, respectively. The solid lines in D are also linear fits on the log–log scale with a slope of 0.7578, 0.8192 and 0.7668, respectively. Error bars are obtained from triplicate measurements. Camera setting:  $f = 5.6$ , ISO = 6400 and exposure time = 30 s.

gated with the reporter enzyme (HRP), a HRP conjugation step was performed after detection antibody incubation (through biotin–streptavidin interaction). Due to the high surface-to-volume ratio and short diffusion distance of the capillaries, during the IL-6 ELISA the sample incubation time was shortened to only 15 minutes,<sup>21,28</sup> and the incubation time for the detection antibody and HRP was also shortened significantly to 12 minutes and 7 minutes, respectively. Furthermore, the quadruplicated rinsing took only 1.5 minutes. Altogether, the total assay time from sample addition to final reading was reduced to only 40 minutes, approximately 8 times faster than 320 minutes needed for the traditional 96-well plate based ELISA according to the manufacturer's protocol (see the ESI†).

The capillary-based ELISA measurements of IL-6 in buffer solution (1% BSA in PBS) and human serum are shown in Fig. 3B and C, respectively. The linear dynamic range is 1–1000 pg ml<sup>-1</sup> and 3–1000 pg ml<sup>-1</sup> for IL-6 in buffer and human serum, respectively. The response curves generated with buffer solution and human serum also appear to have high consistency with each other (the comparison plot can be found in Fig. S3†). For comparison, Fig. 3B and C also plot the ELISA measurements of the same IL-6 samples using traditional 96-well plates and an ELISA reader (PerkinElmer EnSpire 2300 multimode plate reader), showing that, despite an 8-fold reduction in assay time (40 minutes *vs.* 320 minutes) and a 5-fold reduction in sample/reagent volume (20  $\mu$ l *vs.* 100  $\mu$ l), our capillary-based microfluidic ELISA system is able to generate results comparable to 96-well plate based chemiluminescent ELISA. In addition, the capillary based ELISA was found to have good reproducibility among assays performed on different days. Fig. 3D indicates that the slopes of the

regression lines for different IL-6 assays are very close to each other. The slopes are within the range of  $0.781 \pm 0.033$  on the log–log scale, which means the SD  $\leq \pm 4.24\%$  of the average slope.

To validate broader applicability of the capillary based microfluidic ELISA system, we further chose Creatine Kinase-isoform MB (CK-MB), a diagnostic/prognostic marker for myocardial infarction, as the second analyte. Since myocardial infarction is a progressive aggravating deadly disease, rapid quantification of the CK-MB level in serum is crucial to saving patient's life. To further reduce the assay time, we pre-conjugated HRP molecules on the detection antibodies (by amino group crosslinking) with approximately four HRP molecules for one antibody molecule. The revised protocol for CK-MB measurement is illustrated in Fig. 4A, showing the total assay time of only 16 minutes.

The capillary based ELISA measurements of CK-MB in buffer solution (1% BSA in PBS) and human serum are shown in Fig. 4B and C, respectively, showing the linear dynamic range on the log–log scale of 0.1–30 ng ml<sup>-1</sup> and 0.3–30 ng ml<sup>-1</sup>. For comparison, Fig. 4B and C also plot the ELISA measurements of the same CK-MB samples using traditional 96-well plates and an ELISA reader (which requires a total assay time of 210 minutes and 100  $\mu$ l sample/reagent volume). Note that due to the existence of background CK-MB ( $\sim 1$  ng ml<sup>-1</sup>) in human serum, a sudden change in the slope for both capillary and traditional ELISA is observed near the lower end of the CK-MB concentration in Fig. 4C. The background subtracted curves are shown in Fig. S4,† showing a linear response on the log–log scale. In both Fig. 4B and C, the clinically relevant range of CK-MB concentration in serum is marked with grey shades for normal people (0.2–4 ng ml<sup>-1</sup>)

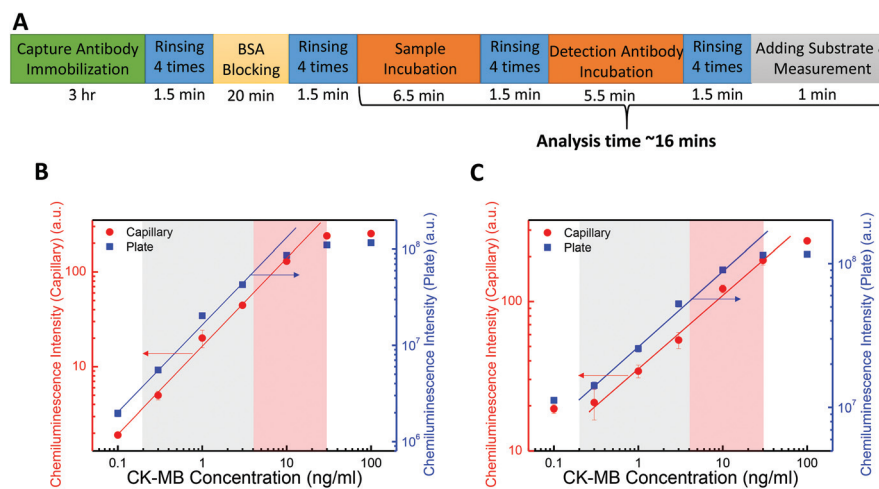


**Fig. 4** (A) Protocol of CK-MB ELISA in capillary reactors. In this case, HRP was pre-conjugated on the detection antibody. The total assay time is around 16 minutes. (B) Response curves of CK-MB ELISA in buffer solution with capillary reactors and a 96-well plate. (C) Response curves of CK-MB ELISA in human serum with capillary reactors and a 96-well plate. Grey shaded areas indicate the range for normal people and red shaded areas indicate the range for myocardial infarction patients. Red lines in B and C are the linear fit for the data collected with capillary reactors on the log-log scale with a slope of 0.8653 and 0.4922, respectively. Blue lines in B and C are the linear fit of the data collected with a 96-well plate on the log-log scale with a slope of 0.8352 and 0.5394, respectively. Error bars are obtained from triplicate measurements. Camera setting:  $f = 7.1$ , ISO = 4000, and exposure time = 30 s.

and red shades for patients with myocardial infarction ( $4\text{--}32 \text{ ng ml}^{-1}$ ),<sup>29,30</sup> which is well in agreement within the linear response range of the capillary based ELISA system.

Our final task in the development of the capillary based ELISA system is to extend its linear dynamic range. Here we used CK-MB in Fig. 4 as the model system to illustrate our approach. Fig. 4B and C show that saturation occurs near the upper end of each response curve, which is caused by the long exposure time of the camera. Fig. S5† suggests that the response of the CMOS on the camera remains linear when the light intensity is between 0 and 160 counts and starts to level

off beyond 160 counts. Therefore, if we keep the intensity counts below 160 using different exposure times, the linear dynamic range can be extended.

In our experiment, we utilized the double-exposure method, in which the emission intensity was recorded with 5 seconds of exposure followed by 30 seconds of exposure. Since the emitting light intensity from the substrate remains stable over a few minutes (which is guaranteed by the manufacturer and validated by our own experiments), the intensity counts can be converted between the two exposures using a factor of 6. The two insets in Fig. 5A show the response curves for lower

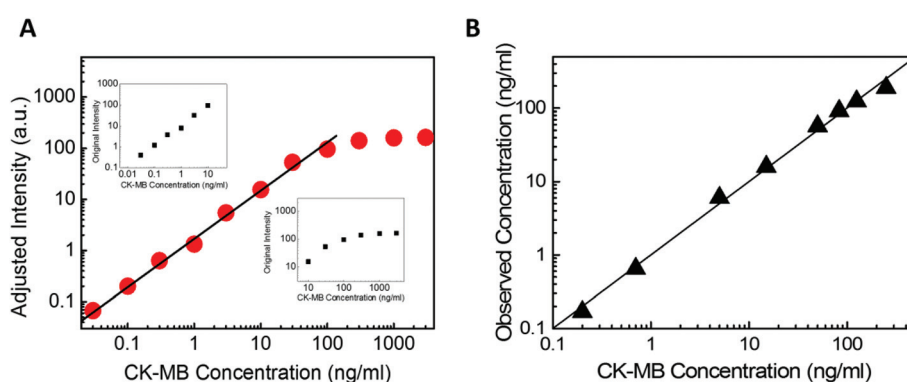


**Fig. 5** (A) Combined CK-MB response curve generated with the double-exposure method (measured in buffer solution). It is adjusted to 5-second exposure time. The dynamic range was extended from less than three orders of magnitude to approximately four orders of magnitude ( $0.03\text{--}200 \text{ ng ml}^{-1}$ ). The solid curve is the linear fit on the log-log scale with a slope of 0.95. Left inset: CK-MB response curve in the low concentration range ( $0.03\text{--}10 \text{ ng ml}^{-1}$ ) with an exposure time of 30 seconds. Right inset: CK-MB response curve in the high concentration range ( $10\text{--}3000 \text{ ng ml}^{-1}$ ) with an exposure time of 5 seconds. (B) The measured CK-MB concentrations using the capillary based ELISA and the data in A as the calibration curve agree well with the expected value. The solid line indicates the ideal reading (i.e., slope = 1) within the concentration range of  $0.1\text{--}500 \text{ ng ml}^{-1}$ .

(0.03–10 ng ml<sup>-1</sup>) and higher (10–3000 ng ml<sup>-1</sup>) CK-MB concentration ranges with the exposure time of 30 seconds and 5 seconds, respectively. The whole response curve can be established in Fig. 5A by combining these two curves after adjusting the 30-second intensity to that for 5-second exposure. Using this combined response curve as the calibration curve and the double exposure method, the CK-MB concentrations in 8 unknown samples were measured and plotted in Fig. 5B. Our results show that the linear dynamic range for CK-MB can easily be extended approximately 10-fold while maintaining good accuracy (although at 250 ng ml<sup>-1</sup>, the accuracy is lowered to  $\pm 20\%$ ).

## Summary

In this work, we demonstrated the performance and applicability of a glass capillary based microfluidic ELISA technique. As summarized in Table S1,<sup>†</sup> our work significantly reduced the required assay time and sample volume in comparison to the traditional plate based ELISA. Furthermore, when the double exposure method is used, the dynamic range can be increased 10-fold.

Our work provides a powerful tool to a broad range of clinical and research/development laboratorial applications. Its short assay time and large dynamic range will enable rapid quantification of the serum level of clinically important biomarkers such as C-reactive protein (CRP), troponin I, troponin T and glial fibrillary acidic protein (GFAP), thus benefitting the diagnosis and prognosis of rapid-developing diseases such as sepsis, acute organ rejection, myocardial infarction and traumatic brain injury. In addition to clinical applications, our small sample volumes can help save precious biological samples for fundamental biological research (such as mouse's tail vein blood and mouse's cerebrospinal fluid) and avoid the necessity of sample dilution, thus reducing the error caused by pipetting.

However, we note that our current design relies on a commercial SLR camera, which made the detection system relatively bulky. In addition, the distance between the camera and capillary reactors was still too far. Further miniaturization and customization of the imaging system are needed to make the device more practically viable.

## Acknowledgements

We thank the support from the National Science Foundation (DBI-1451127).

## References

- 1 H. Matsumoto, S. Shinzaki, M. Narisada, S. Kawamoto, K. Kuwamoto, K. Moriwaki, F. Kanke, S. Satomura, T. Kumada and E. Miyoshi, *Clin. Chem. Lab. Med.*, 2010, **48**, 505.
- 2 R. M. Lequin, *Clin. Chem.*, 2005, **51**, 2415–2418.
- 3 E. Engvall and P. Perlmann, *Immunochemistry*, 1971, **8**, 871–874.
- 4 S. K. Vashist, P. B. Luppa, L. Y. Yeo, A. Ozcan and J. H. Luong, *Trends Biotechnol.*, 2015, **33**, 692–705.
- 5 S. K. Vashist, T. van Oordt, E. M. Schneider, R. Zengerle, F. von Stetten and J. H. Luong, *Biosens. Bioelectron.*, 2015, **67**, 248–255.
- 6 B. Berg, B. Cortazar, D. Tseng, H. Ozkan, S. Feng, Q. Wei, R. Y.-L. Chan, J. Burbano, Q. Farooqui and M. Lewinski, *ACS Nano*, 2015, **9**, 7857–7866.
- 7 L.-J. Wang, Y.-C. Chang, R. Sun and L. Li, *Biosens. Bioelectron.*, 2017, **87**, 686–692.
- 8 E. Eteshola and D. Leckband, *Sens. Actuators, B*, 2001, **72**, 129–133.
- 9 M. Herrmann, E. Roy, T. Veres and M. Tabrizian, *Lab Chip*, 2007, **7**, 1546–1552.
- 10 T. Wang, M. Zhang, D. D. Dreher and Y. Zeng, *Lab Chip*, 2013, **13**, 4190–4197.
- 11 S. K. Vashist, O. Mudanyali, E. M. Schneider, R. Zengerle and A. Ozcan, *Anal. Bioanal. Chem.*, 2014, **406**, 3263–3277.
- 12 J. Kai, A. Puntambekar, N. Santiago, S. H. Lee, D. W. Sehy, V. Moore, J. Han and C. H. Ahn, *Lab Chip*, 2012, **12**, 4257–4262.
- 13 B. S. Lee, J.-N. Lee, J.-M. Park, J.-G. Lee, S. Kim, Y.-K. Cho and C. Ko, *Lab Chip*, 2009, **9**, 1548–1555.
- 14 R. Gorkin, J. Park, J. Siegrist, M. Amasia, B. S. Lee, J.-M. Park, J. Kim, H. Kim, M. Madou and Y.-K. Cho, *Lab Chip*, 2010, **10**, 1758–1773.
- 15 B. S. Lee, Y. U. Lee, H.-S. Kim, T.-H. Kim, J. Park, J.-G. Lee, J. Kim, H. Kim, W. G. Lee and Y.-K. Cho, *Lab Chip*, 2011, **11**, 70–78.
- 16 M. Garcia, J. Orozco, M. Guix, W. Gao, S. Sattayasamitsathit, A. Escarpa, A. Merkoci and J. Wang, *Nanoscale*, 2013, **5**, 1325–1331.
- 17 M. Herrmann, T. Veres and M. Tabrizian, *Lab Chip*, 2006, **6**, 555–560.
- 18 T. Ohashi, K. Mawatari, K. Sato, M. Tokeshi and T. Kitamori, *Lab Chip*, 2009, **9**, 991–995.
- 19 X. Weng, G. Gaur and S. Neethirajan, *Biosensors*, 2016, **6**, 24.
- 20 S. Wang, L. Ge, X. Song, J. Yu, S. Ge, J. Huang and F. Zeng, *Biosens. Bioelectron.*, 2012, **31**, 212–218.
- 21 E. Tsutsumi, T. G. Henares, S.-i. Funano, K. Kawamura, T. Endo and H. Hisamoto, *Anal. Sci.*, 2012, **28**, 51–51.
- 22 T. G. Henares, E. Tsutsumi, H. Yoshimura, K. Kawamura, T. Yao and H. Hisamoto, *Sens. Actuators, B*, 2010, **149**, 319–324.
- 23 S.-i. Funano, M. Sugahara, T. G. Henares, K. Sueyoshi, T. Endo and H. Hisamoto, *Analyst*, 2015, **140**, 1459–1465.
- 24 S.-i. Funano, T. G. Henares, M. Kurata, K. Sueyoshi, T. Endo and H. Hisamoto, *Anal. Biochem.*, 2013, **440**, 137–141.
- 25 W.-J. Kim, S. H. Hyun, H. Y. Cho, S. Byun, B. K. Kim, C. Huh, K. H. Chung and Y. J. Kim, *Sens. Actuators, B*, 2016, **233**, 281–288.

- 26 R. Huda, D. R. Solanki and M. Mathru, *Clin. Sci.*, 2004, **107**, 497–503.
- 27 A. N. Vgontzas, D. A. Papanicolaou, E. O. Bixler, A. Kales, K. Tyson and G. P. Chrousos, *J. Clin. Endocrinol. Metab.*, 1997, **82**, 1313–1316.
- 28 K. Sato, M. Tokeshi, T. Odake, H. Kimura, T. Ooi, M. Nakao and T. Kitamori, *Anal. Chem.*, 2000, **72**, 1144–1147.
- 29 J. F. Saucedo, R. Mehran, G. Dangas, M. K. Hong, A. Lansky, K. M. Kent, L. F. Satler, A. D. Pichard, G. W. Stone and M. B. Leon, *J. Am. Coll. Cardiol.*, 2000, **35**, 1134–1141.
- 30 S. Fuchs, R. Kornowski, R. Mehran, A. J. Lansky, L. F. Satler, A. D. Pichard, K. M. Kent, C. E. Clark, G. W. Stone and M. B. Leon, *Am. J. Cardiol.*, 2000, **85**, 1077–1082.